Mechanism, dynamics, and biological existence of multistability in a large class of bursting neurons

Cite as: Chaos **20**, 023118 (2010); https://doi.org/10.1063/1.3413995
Submitted: 02 November 2009 . Accepted: 06 April 2010 . Published Online: 17 June 2010

Jonathan P. Newman, and Robert J. Butera

Mechanism, dynamics, and biological existence of multistability in a large class of bursting neurons

Jonathan P. Newman[a] and Robert J. Butera[b]
Wallace H. Coulter Department of Biomedical Engineering, Georgia Institute of Technology, Atlanta, Georgia 30332-0535, USA

(Received 2 November 2009; accepted 6 April 2010; published online 17 June 2010)

Multistability, the coexistence of multiple attractors in a dynamical system, is explored in bursting nerve cells. A modeling study is performed to show that a large class of bursting systems, as defined by a shared topology when represented as dynamical systems, is inherently suited to support multistability. We derive the bifurcation structure and parametric trends leading to multistability in these systems. Evidence for the existence of multirhythmic behavior in neurons of the aquatic mollusc *Aplysia californica* that is consistent with our proposed mechanism is presented. Although these experimental results are preliminary, they indicate that single neurons may be capable of dynamically storing information for longer time scales than typically attributed to nonsynaptic mechanisms. © *2010 American Institute of Physics*. [doi:10.1063/1.3413995]

Neurons that support bursting dynamics are a common feature of neural systems. Due to their prevalence, great effort has been devoted to understanding the mechanisms underlying bursting and information processing capabilities that bursting dynamics afford. In this paper, we provide a link between neuronal bursting and information storage. Namely, we show that the mechanism implicit to bursting in certain neurons may allow near instantaneous modifications of activity state that lasts indefinitely following sensory perturbation. Thus, the intrinsic, extrasynaptic state of these neurons can serve as a memory of a sensory event.

I. INTRODUCTION

Bursting is a dynamic state characterized by alternating periods of fast oscillatory behavior and quasi-steady-state activity. Nerve cells commonly exhibit autonomous or induced bursting by firing discrete groups of action potentials in time. Autonomously bursting neurons are found in a variety of neural systems, from the mammalian cortex[1] and brainstem[2–4] to identified invertebrate neurons.[5,6]

Multirhythmicity in a dynamical system is a specific type of multistability which describes the coexistence of two or more oscillatory attractors under a fixed parameter set. Multirhythmicity has been shown to occur in vertebrate motor neurons,[7] invertebrate interneurons,[8] and in small networks of coupled invertebrate neurons.[9] Additionally, multirhythmicity has been demonstrated in models of intracellular calcium oscillations[10] and coupled genetic oscillators.[11]

Multistable systems can act as switches in response to an external input. The feasibility of multistability as an information storage and processing mechanism in neural systems has been widely discussed in terms of neural recurrent loops and delayed feedback mechanisms.[12–14] Theoretical studies have shown multirhythmic bursting behavior in a number of single neuron models[15,16] as well as in a model two-cell inhibitory (half-center oscillator) network.[17] In biological neurons, it is possible that these dynamics are employed as a short term memory. This report provides a general explanation for the existence of multirhythmic bursting in previous studies[15,16,18] and the characteristics of a bursting neuron that allow multirhythmic dynamics. Additionally, we provide experimental evidence, suggesting the existence of this behavior in several identified bursting neurons of the aquatic mollusc *Aplysia californica*.

II. A SIMPLE PARABOLIC BURSTING MODEL

Dynamical bursting systems are a subset of the singularly perturbed (SP) class of differential equations,

$$\dot{x} = f(x,y), \tag{1}$$

$$\dot{y} = \epsilon g(x,y), \quad x \in \mathbf{R}^m, \quad y \in \mathbf{R}^n, \tag{2}$$

where $0 \leq \epsilon$ is a small parameter. Using singular perturbation methods,[19,20] the dynamics of bursting models can be explored by decomposing the full system into fast and slow subsystems: Eqs. (1) and (2), respectively. The slow subsystem can act independently,[21] be affected synaptically,[17] or interact locally with the spiking fast subsystem[5,15–17] to produce alternating periods of spiking and silence in time. To examine the dynamical mechanism implicit to a bursting behavior, y is treated as a bifurcation parameter of the fast subsystem. This is formally correct when $\epsilon = 0$ and Eq. (2) degenerates into an algebraic equation, but the assumption is reasonable when there is a large time separation between fast and slow dynamics.

Using this technique, all autonomously bursting single neuron models displaying multirhythmic bursting in

[a]Electronic mail: jnewman6@gatech.edu.
URL: http://www.prism.gatech.edu/~jnewman6.
[b]Electronic mail: rbutera@gatech.edu. Also at School of Electrical and Computer Engineering, Georgia Institute of Technology, Atlanta, Georgia 30332-0250.

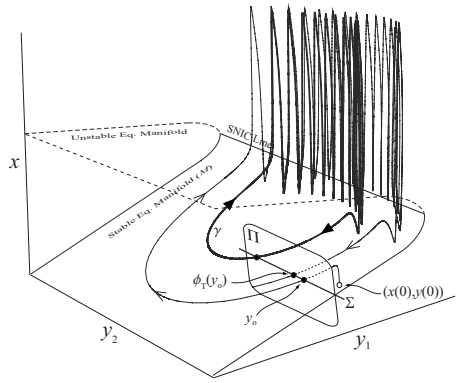

FIG. 1. A generic circle/circle bursting system projected into $\mathbf{R}^{1+2}$. The dynamics of x is much faster than that of y. At some points, trajectories are smashed onto the fast equilibrium manifold, allowing return maps created from Poincaré sections of dimension $n-1$ to provide a complete dynamical description of the continuous system (see text for details).

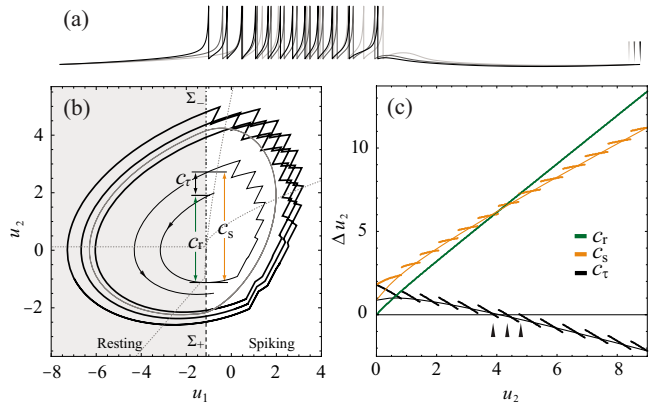

FIG. 2. (Color online) Multirhythmic bursting produced by Eqs. (3)–(5). (a) Voltage traces showing a single period of three coexisting, limit cycles of 10, 11, and 12 spikes. Note that the period of coexisting bursting solutions is different as indicated by three endpoint markers. (b) The corresponding limit cycles projected into the plane of the slow variables (thick) with the averaged solution shown in gray. Dotted gray lines are the nullclines of the averaged bursting system [see Eqs. (13) and (14)]. Contraction metrics, C_r, C_s, and C_τ [Eqs. (9)–(11)] are demonstrated on a portion of a trajectory of the full system spiraling outward (thin). The dashed line (Σ_+) and dot-dashed line (Σ_-) are the Poincaré sections used to define G and H [Eqs. (6) and (7)]. (c) C_r, C_s, and C_τ for the multirhythmic system in (a). When the contraction of the slow focus is balanced by expansive spiking events, $C_\tau=0$ and there is a fixed point of the map. Contraction metrics for the averaged system are thin solid lines. Parameters used here are $I=0.5$ ($I=1.2$ for averaged system), $\alpha=0.2$, $\beta=0.05$, $d_1=0.4$, $d_2=0.6$, $v_c=10$, and $v_r=-1$.

literature[15,16] are topologically classified as the circle/circle type;[22,23] that is, their fast subsystem is driven back and forth across a saddle node on invariant circle (SNIC) bifurcation to produce alternating spiking and silent states. These models can be reduced to a form that supports a topological normal SNIC to and from the active phase.[23] This system is

$$\dot{v} = I + v^2 + u_1, \tag{3}$$

$$\dot{u}_1 = -\alpha u_2, \tag{4}$$

$$\dot{u}_2 = -\beta(u_2 - u_1), \tag{5}$$

where I is a constant current, and α and β are small positive constants. Trajectories are reset after a voltage spike by $v=v_c, v \leftarrow v_r$ and $(u_1,u_2) \leftarrow (u_1+d_1, u_2+d_2)$, where $v_c - v_r$, and d_1 and d_2 are discrete shifts in variables that account for the effects of a spike. Thus, the slow subsystem defined by Eqs. (4) and (5) is a damped linear oscillator defining a stable focus when $\beta < 4\alpha$ or node when $\beta \geq 4\alpha$. Under the parameter sets used here, the slow subsystem is a focus. Equation (3) is the fast subsystem and is a quadratic integrate and fire neuron.

Equations (3)–(5) are SP systems for small α and β. When u_1 is used as a bifurcation parameter of the singular system [Eq. (3)], a saddle node bifurcation occurs when $u_1 = u_{sn} = -I$. When $u_1 > u_{sn}$, $v \to \infty$ like $\tan(t)$ (see Appendix A 1). In the full system, when $u_1 < u_{sn}$, trajectories slowly converge on the equilibrium point of the slow focus. When $u_1 > u_{sn}$, trajectories of the slow subsystem are interrupted by spiking events when v goes to v_c and (u_1,u_2) are discretely modified. The existence of a bursting solution is reliant on the interaction between spiking events and a flow of the slow focus—neither activity type can exist indefinitely when isolated. A necessary condition for the existence of a limit cycle that represents bursting or tonic spiking is that the equilibrium point of the slow subsystem (u_1^*, u_2^*) must satisfy $u_1^* > u_{sn}$.

A general aspect of SP systems of the form [Eqs. (1) and (2)] is that if $M = \{(x,y) | f(x,y) = 0\}$ is a stable equilibrium manifold of the fast subsystem on which $D_x f$ is nonsingular, trajectories on M follow the reduced field, $\dot{y} = g(h(y),y)$, where $h(y)$ is a function satisfying $f(h(y),y) = 0$.[24] With this in mind, consider an $m+n$ dimensional circle/circle bursting system [e.g., Eqs. (3)–(5)]. Let ϕ_t be the flow of the full system. On M, $h(y)$ is dependent on y and static parameters. With $\epsilon = 0$, $\phi_t(x,y) = \phi_t(h(y),y)$ since the time scales of the singular and slow subsystem are assumed to have infinite separation. Hence, if local cross section $\Pi \subset \mathbf{R}^{m+n}$ of dimension $m+n-1$ is everywhere transverse to ϕ_t, the condition $\phi_\tau(h(y_0),y_0) = (h(y_0),y_0)$ on Π shows a τ-periodic closed orbit. This condition reduces to $\phi_\tau(y_0) = y_0$ and fixed points of a $n-1$ dimensional map generated from an $n-1$ dimensional section on M show closed orbits in $\mathbf{R}^{m+n}$ (Fig. 1). In the case of Eqs. (3)–(5), $n=2$. Therefore, a one-dimensional return map equivalent to the full system can be created using a one-dimensional section Σ.

III. BURSTING SOLUTIONS RESULT FROM COUNTERACTING DYNAMICS

Figure 2 indicates that discrete spiking events on a circle/circle bursting solution have a contraction-balancing action in phase space; they periodically force the stable focus, returning it to its initial condition after a single period, and transforming the focal trajectory into a limit cycle. When trajectories containing *different numbers* of spiking events return to their initial condition after a full revolution, multiple coexisting limit cycles are formed and multirhythmic bursting is achieved.

Consider multirhythmic bursting produced by Eqs. (3)–(5) in Fig. 2. Let M_c represent the equilibrium manifold of Eq. (3) parametrized by u_1. We recall from Sec. II that an $n-1=1$ dimensional section is needed to form a return map

for the system defined by Eqs. (3)–(5) so long as that section is on M_c. Therefore, we can define this section as the line of saddle nodes that divide the silent and spiking regimes of phase space, $\Sigma_c=\{(u_1,u_2)\in\mathbf{R}|u_1=u_{sn}\}$. Consequently, a one-dimensional recurrence map, $P:u_2\rightarrow u_2$, is formed by intersections with the Poincaré section,[25]

$$\Sigma_- \equiv \{(u_1,u_2)\in\mathbf{R}|u_1\in\Sigma_c,\dot{u}_1<0\}. \tag{6}$$

To further explain how bursting and multirhythmicity arises in circle/circle systems, we divide the full return map P into two components, G and H, in terms of two Poincaré sections, Σ_-, and an additional section,

$$\Sigma_+ \equiv \{(u_1,u_2)\in\mathbf{R}|u_1\in\Sigma_c,\dot{u}_1>0\}. \tag{7}$$

Here, G is a mapping from some initial condition, $u_2(0)\in\Sigma_-$, to a point on Σ_+. H is then a mapping from $G(u_2(0))$ back to Σ_- (Fig. 2). Thus, over the course of a periodic trajectory, G accounts for the dynamics in the silent (contractive) region to the left of Σ_c and H accounts for the dynamics in the spiking (expansive) region to the right of Σ_c. The functional composition of these maps,

$$P(u_2)=H(G(u_2)), \tag{8}$$

is the discrete time Poincaré recurrence map as previously defined. Using G and H, distance metrics,

$$C_r(u_2)=u_2-G(u_2), \tag{9}$$

$$C_s(u_2)=G(u_2)-H(u_2), \tag{10}$$

$$C_\tau(u_2)=C_s(u_2)-C_r(u_2) \tag{11}$$

can be compared to describe contraction of trajectories in the resting, spiking, and combined regions of state space, respectively (see Fig. 2). For points $u_2^*\in\Sigma_-$ that $C_\tau(u_2^*)=0$, the contraction of the resting portion of the trajectory is balanced by the net expansion of the spiking portion. Hence, u_2^* are fixed points of P and therefore show closed orbits in the full system.

Contraction and expansion of Eqs. (3)–(5) are clarified by examining the averaged slow subsystem. This uses a near-identity change of variables to account for the time-averaged effect of fast spiking when $u_1>u_{sn}$. Let $\varphi(t,u)$ be the limit cycle of the fast subsystem defining T-periodic spiking. $\dot{u}=\epsilon g(\varphi(t,u),u)$ is the periodically forced slow subsystem. By the Pontryagin–Rodygin theory,[26] the averaged slow subsystem for $u_1>u_{sn}$ is defined as

$$\dot{z}=\frac{\epsilon}{T(z)}\int_0^{T(z)} g(\varphi(t,z),z)dt, \tag{12}$$

where $z=u+\mathcal{O}(\epsilon)$. So, for our simple model, the averaged slow subsystem is the switched system,

$$\dot{z}_1=\begin{cases} -\alpha z_2 & \text{if } z_1\le u_{sn} \\ -\alpha z_2+\dfrac{d_1}{T(z_1)} & \text{if } z_1>u_{sn}, \end{cases} \tag{13}$$

$$\dot{z}_2=\begin{cases} -\beta(z_2-z_1) & \text{if } z_1\le u_{sn} \\ -\beta(z_2-z_1)+\dfrac{d_2}{T(z_1)} & \text{if } z_1>u_{sn}, \end{cases} \tag{14}$$

where

$$T(z_1)=\frac{1}{\sqrt{z_1+u_{sn}}}\left(\arctan\left(\frac{v_c}{\sqrt{z_1+u_{sn}}}\right)-\arctan\left(\frac{v_r}{\sqrt{z_1+u_{sn}}}\right)\right) \tag{15}$$

(see Fig. 2 and Appendix A). Now opposing contraction dynamics are explicit between terms on the right hand side of Eqs. (13) and (14) when $z_1>u_{sn}$.

IV. CONDITIONS FOR MULTIRHYTHMICITY

Nonmonotonicity of C_τ is a necessary condition for multirhythmic bursting in circle/circle models because it means that P may support several isolated contraction mappings. Fluctuations in the contraction of P as measured by C_τ are the result of near quantal spike addition in the active phase of bursting. Because the averaged system produces a monotonic C_τ, it cannot generate a saddle node bifurcation of closed orbits (SCOs) and therefore cannot support multiple coexisting stable solutions.

Consider a closed orbit of the simple model γ projected into the plane (u_1,u_2) containing N spiking events. The dynamics on trajectories originating on the plane inside γ is dominated by expansive spiking and they spiral outward. The dynamics on trajectories originating outside γ is dominated by contraction of the focus and they spiral inward. However, when initial condition $(u_1(0),u_2(0))$ lies some critical distance outside γ, the arc length of the resulting trajectory past u_{sn} is long enough such that it contains $N+1$ spikes and its dynamics may become net expansive, causing it to spiral outward, indicating a "jump" in C_τ. If this occurs, this trajectory forms the inner boundary of the trapping region of a second oscillatory attractor. Since in Eqs. (13) and (14) quantal spiking is averaged over time, divisions between expansive and contractive annuluses about the equilibrium point are lost and P is a single contraction mapping for all initial conditions [Fig. 2(c)].

Concentric basins of attraction in the plane must be divided by an unstable invariant set. In Eqs. (3)–(5), unstable periodic orbits (UPOs) are merely conceptual since spike addition occurs in a strictly discrete fashion. For a continuous system, UPOs form separatixes for concentric basins of attraction. They are closed orbits that contain a dynamically unlikely attenuated action potential in the active phase. This can be seen in the biophysical models that support multirhythmic bursting.[15,16] UPOs in these systems correspond to the unstable fixed points of P which separate contraction mappings.

C_τ is nonmonotonic for Eqs. (3)–(5), so moving toward some parameter sets causes its local minima and maxima to cross zero, indicating the creation or annihilation of a stable/unstable orbit pair via a SCO. The damping ratio of the slow subsystem is $\zeta=\beta/2\sqrt{\alpha\beta}$. As damping is reduced in the slow

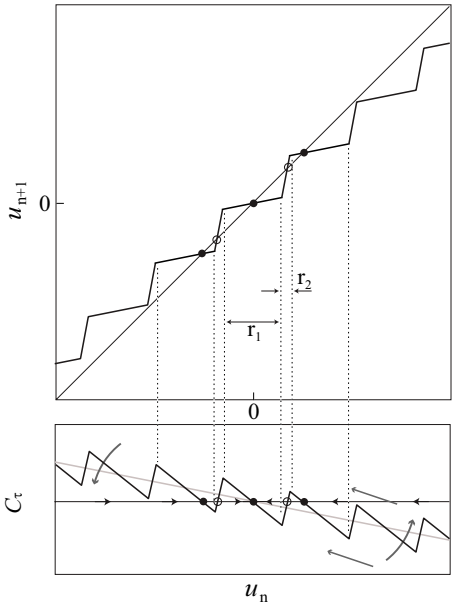

FIG. 3. (Color online) An idealization of P and C_τ for a circle/circle bursting model with a slow variable u. Stable and unstable fixed points are filled and open dots, respectively. The slow subsystem becomes less dissipative and spiking events are capable of balancing contraction over larger areas of phase space. This effectively decreases the average slope of C_τ, leading to the formation of multiple fixed points via SCOs (curved arrows). Parametric changes that drive trajectories of the slow subsystem further past u_{sn} cause the number of spikes during an active phase to be increasingly sensitive to the initial condition. This effectively compresses C_τ, increasing the number of separate contraction mappings via SCOs (straight arrows). P has three separate contraction mappings over the three sets of preimages within the dotted lines.

subsystem by $\beta \to 0$ and $\alpha \to \infty$, the dynamics moves toward quasistable. This effectively reduces the average slope of C_τ, pushing more of its extrema across zero, causing SCOs to occur. Additionally, in circle/circle bursting systems, the firing rate past the SNIC scales as $\sqrt{b-b_{sn}}$, where b is the bifurcation parameter and b_{sn} is its value at the saddle node bifurcation [e.g., Eq. (15) for the simple model]. Since $|\dot{u}_1/\dot{u}_2|$ increases as $\alpha \to \infty$ and $\beta \to 0$, flow increases into u_1 following these parameter limits. This allows spike addition to occur more readily as a function of the initial condition (Fig. 3).

An interesting consequence of the mechanism underlying multirhythmic bursting in the simple model is that as $\alpha \to \infty$ and $\beta \to 0$ and when d_1 and d_2 are sizable, arbitrarily many stable bursting solutions can coexist.

V. CLASSIFICATION OF POSSIBLE BURSTING BEHAVIORS

From Sec. IV, it is apparent that a circle/circle bursting system can be reduced to a one-dimensional map that switches between two modes. This can be verified for complicated models of circle/circle bursting which produce highly nonlinear return maps, but preserve an alternating, sawtoothlike structure.[16]

To explore the dynamics possible under this constraint, we introduce a simple piecewise linear map acting on a slow variable u that is depicted in Fig. 3, top. Starting with a local contraction mapping symmetric about the origin, the map

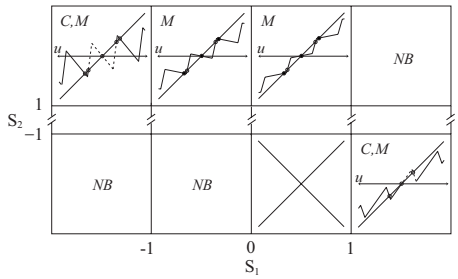

FIG. 4. Examples of the maps corresponding to the different parameter sets outlined in Table I. Qualitative dynamics are classified by the following symbols: M—may support multirhythmicity, C—chaotic, and NB—nonbiological. Dashed sections of the maps show a single link in a chain of chaotic maps (sawtooth or tent map). The block for $0<s_1<1$, $s_2<-1$, is crossed out because the resulting map is not well defined.

alternates in both directions between two moduli, s_1 and s_2, which act over sets of sizes r_1 and r_2, respectively. Since the map defined by $u_{n+1}=s_1 u_n$ is a contraction mapping, we confine $|s_2|>1$ so that it is possible to have multiple basins of attraction. The average slope of the map is given by $s_{av}=(s_1 r_1+s_2 r_2)/(r_1+r_2)$. $|s_{av}|<1$ requires the existence of at least one attractor under the map. Compared to P, the map is translated so that a central fixed point is located at the origin. Therefore, we consider the fixed point at the origin a nominal bursting solution with N spikes. Jumps to different contraction mappings indicate jumps to new bursting solutions with $N \pm k$, $k=1,2,3,\ldots$ spikes in the active phase.

Now the limiting behavior of circle/circle bursting can be explored by inspecting the map for different values of s_1 and s_2. This analysis is carried between Fig. 4 and Table I. We note that the range of behaviors described by this simple system account for all the dynamics reported in previous multirhythmic bursting studies[15,16] including the coexistence of chaotic attractors. However, those models are not topologically conjugate to our piecewise linear map since they can produce combinations of limit sets seen in different parameter regimes of the one-dimensional system under a single parameter set (e.g., the coexistence of a limit cycle and a strange attractor).

VI. MULTIRHYTHMIC BURSTING IN BIOLOGICAL NEURONS

We now provide evidence for the existence of multirhythmicity and multirhythmic bursting in invertebrate interneurons and neurosecretory cells. Cells R15, L3-L6, and L10 are identified neurons (neurons that are preserved animal to animal) located in the abdominal ganglion of *Aplysia californica*. These neurons burst spontaneously *in situ* with or without synaptic isolation. Additionally, they display the "parabolic" bursting type, as distinguished by two key features. First, they are characterized by root scaling in firing rate during the active phase (Fig. 5). Second, action potentials during bursting have afterhyperpolarizations that are lower than the voltage threshold for the active phase, ruling out a hysteresis mechanism for bursting.[19] Therefore, we can conclude that the circle/circle type mechanism for bursting well describes their dynamics.

TABLE I. The qualitative behavior of the piecewise linear map shown in Fig. 4 is described for each parameter regime. The top section describes why some parameter values are irrelevant to our analysis. The bottom section describes relevant parameter ranges that can fully account for the dynamics witnessed in prior multirhythmic bursting models.

s_1	s_2	Dynamics
⋯	$\lvert s_2\rvert<1$	s_2 must have modulus greater than 1
$\lvert s_1\rvert<1$	$s_2<-1$	Nonbiological because $s_{av}<0$
$s_1>1$	$s_2>1$	Nonbiological because $s_{av}>1$ indicating that the system is a repeller
$0<s_1<1$	$s_2<-1$	Map is not well defined
$s_1<-1$	$s_2>1$	Chaotic and possibly multirhythmic since the full map is formed by a chain of sawtooth maps with only unstable fixed points
$-1<s_1<0$	$s_2>1$	Attractors are oscillatory fixed points and the system is possibly multirhythmic
$0<s_1<1$	$s_2>1$	Attractors are nonoscillatory fixed points and the system is possibly multirhythmic
$s_1>1$	$s_2<-1$	Chaotic and possibly multirhythmic since the full map is formed by a chain of tent maps with only unstable fixed points

R15 is the most heavily studied of the aforementioned neurons due to its particularly stable activity and long burst period.[6] Numerous models[5,20,27–29] have attempted to describe the mechanisms underlying bursting in this cell and many of these models are of the circle/circle type.[22] One class of models[16,20,27,29,30] postulates that the slow variables underlying bursting are (1) the degree of voltage-gated activation of a slow, inward Ca^{2+} current I_{SI} and (2) intracellular calcium concentration. Activation of I_{SI} increases intracellular Ca^{2+} and I_{SI} displays voltage dependent activation and Ca^{2+} dependent inactivation.

We used a traditional "current-clamp" technique to control the applied current across the cell membrane, while monitoring the membrane potential. Since I_{SI} and intracellular Ca^{2+} concentration are directly and indirectly voltage dependent, current perturbations that change the membrane potential may influence these variables such that a multirhythmic cell is forced to switch attractors. Specifically, since our hypothesized mechanism of attractor switching involves spike addition, we aimed to change the number of action potentials in the active phase of bursting.

Models of R15 predict that outward current perturbations hyperpolarize the cell from its spiking threshold and when the cell is released from this hyperpolarized state, it spikes vigorously ("rebounds"), leading to spike addition. Since activation of I_{SI} is depolarization dependent, prolonged hyperpolarization completely deactivates Ca^{2+} channels supporting I_{SI}. Additionally, in the absence of an inward Ca^{2+} flux, the intracellular Ca^{2+} concentration decreases due to cytosolic buffering[27] and the ion channels supporting I_{SI} are deinactivated. When the inhibitory current is released, the resulting depolarization quickly activates I_{SI}, allowing it to pass inward Ca^{2+} current which maintains a high membrane potential causing spikes. Since intracellular Ca^{2+} was initially very low, I_{SI} must pass more Ca^{2+} than usual before it is inactivated, resulting in a prolonged active phase. A depolarizing current has an opposing effect. Using 2–8 s, from −0.5 to −2.5 nA hyperpolarizing current perturbations during the silent phase of bursting to add spikes to the subsequent active phase, we were able to show evidence for a multirhythmic behavior in four out of eight bursting cells (see Appendix B for details of the experimental method). Figure 6 shows recordings in two different bursting neurons from separate animals that display a multirhythmic behavior along with the current perturbations used to induce an attractor switch.

Section IV predicts that an attractor switch in a multirhythmic burster will be characterized by spike addition or deletion and an increase or a decrease in burst period, respectively. Figure 7 presents a comparison of slow-wave activity in Fig. 6(b) for two bursts prior and subsequent to the stimulus. Because coexisting bursting solutions are concentric in our models, the path length of the solutions must differ, resulting in distinct periods for each solution [see Fig. 2(a)]. Note that the existence of a constant phase advance developed after spike addition shown in Fig. 7(a) satisfies this

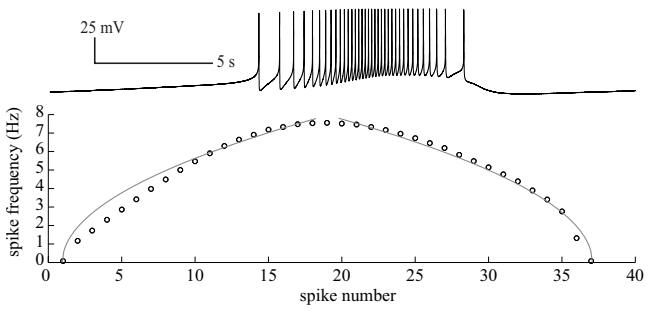

FIG. 5. Early studies of R15 deemed the neuron a "parabolic" burster since the spike-period profile resembles a parabola. However, it is now known that root scaling (gray line) better describes the frequency profile of this shape, since after a SNIC, the period of the resulting limit cycle scales as $1/\sqrt{\lambda}$ [Eq. (15) for the simple model]. This figure confirms that this behavior in an *in situ* recording of R15. The instantaneous spike frequency during the active phase is shown with open circles.

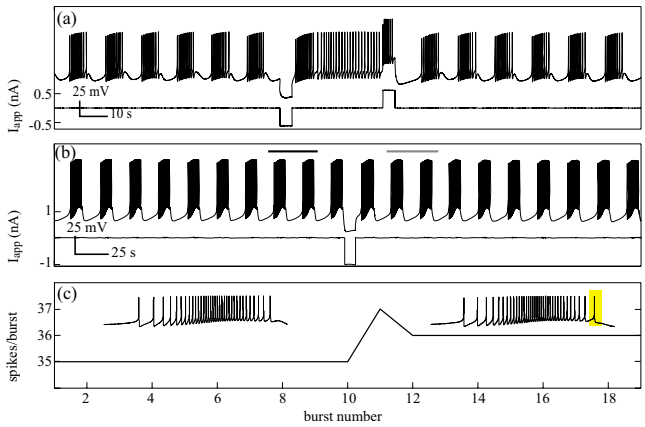

FIG. 6. (Color online) Multirhythmicity in bursting neurons of *Aplysia's* abdominal ganglion. (a) A "left-upper-quadrant" cell, most likely L3, showing bistability between bursting and tonic spiking. This behavior is predicted in biophysical models (Refs. 15 and 31) and was shown previously in R15 (Ref. 8). Fundamentally, it is explained by the one-dimensional map P (Sec. V) with $N=11$ spikes per burst in the nominal (nonperturbed) mode and $N=1$ spike per burst after the current pulse. Applied current pulses likely manipulate intracellular Ca^{2+} concentrations, effectively moving the trajectory about in the plane of the slow variables, and allowing an attractor switch. (b) R15 showing bistability between two bursting solutions. Although the current pulse appears to have little effect, (c) shows the amount of spikes in the active phase of each burst. After the perturbation is applied, the number of spikes per burst increases by 2 and then relaxes onto the new attractor containing 36 spikes per burst. The active phase for pre- and post-perturbation is shown with the added spike highlighted.

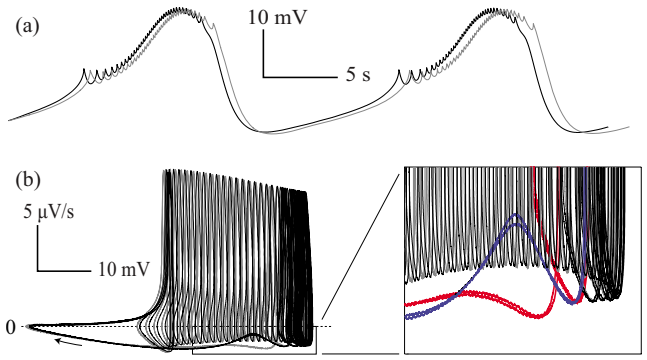

FIG. 7. (Color online) Attractor reconstruction from the experimentally derived voltage traces. (a) Two bursts preceding and subsequent to stimulation were used for a comparative attractor reconstruction [bars in Fig. 6(b) denote the bursts used]. A single burst period was defined by the time between rising edges through −70 mV in the smoothed voltage trace. Voltage time series was low pass filtered using an exponentially weighted moving average with a width of 2 s to prevent spiking events from dominating the reconstructed attractor. Note the constant phase advance of the grey trace in comparison with the black, which is predicted by our model in Fig. 2. (b) Voltage plotted against its estimated derivative. This attractor shape can be directly compared to biophysical models of neurons which rely on a circle/circle bursting mechanism. A zoomed portion of the reconstruction is shown to highlight the existence of a separatix dividing the two attractors, an unstable closed orbit that contains an attenuated spike. The final portion of the active phase is thickened and colored for each attractor to make this clear.

prediction. In an attempt to elucidate the shape of the two coexisting attractors, we plotted voltage versus its estimated derivative in Fig. 7(b). Our multirhythmic model predicts that an unstable bursting solution containing an attenuated spike separates stable solutions. This separatix appears to exist, separating one attractor from the other it proceeds for an additional spike in Fig. 7(c).

One may argue that the current perturbations we provide are too large both temporally in terms of current amplitude to resemble a synaptic effect. However, the volume of charge moved across the membrane is a very superficial definition of synaptic efficacy. Smaller synaptic currents that rely on specific charge carriers (e.g., synaptic activation of calcium-specific channels) can be more effective in terms of altering specific neuron dynamics than our large chloride based currents. In the future, it would be interesting to repeat our experiment with direct perturbations to the hypothesized slow subsystem via intracellular calcium uncaging.

VII. POSSIBLE IMPLICATIONS OF MULTIRHYTHMIC BURSTING

Since the time scales associated with short term memory, for example, the multirhythmic motor memory suggested in Ref. 7 are shorter than those associated with morphological synaptic plasticity, it is possible that neural systems employ some activity dependent multistability as a memory. Most proposed mechanisms of dynamic multistability in neural systems rely on some delayed feedback mechanism in a small neural circuit as the driving force in the creation of multiple coexisting attractors.[12–14] Here, we have shown that a sufficiently underdamped slow subsystem in a single circle/circle bursting neuron is enough to ensure the existence of multirhythmic behavior.

We chose to show the existence of this phenomenon using invertebrate neurons because of their relative ease of experimental manipulation. However, as is put forth in Secs. IV and V, the dynamical mechanism underlying multirhythmic bursting is general and the multirhythmic regime occupies a nonfinite range of parameter space; circle/circle bursting systems appear inherently suited for short term information stor-

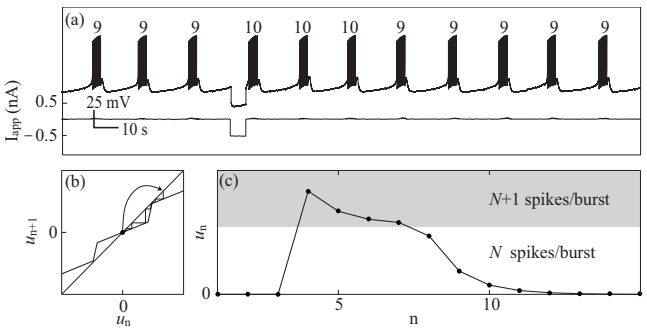

FIG. 8. "Fading" multirhythmicity in L4 of *Aplysia's* abdominal ganglion. (a) Voltage trace and the corresponding current perturbation. The three bursts following the perturbation contain an extra spike. This results from forcing the trajectory to pass through an bottleneck where dynamics is close to fixed, which causes a lasting effect on bursting without the system actually being multirhythmic. (b) Fading multirhythmicity using the piecewise linear representation of P. Note that the map has areas that are close to forming fixed points. A trajectory can temporarily become caught here, allowing a temporal amplification of a small perturbation (curved arrow). (c) Time series of the trajectory in (c). The ruins of a SCO allow the system to maintain $N+1$ spikes per burst for a time before falling back into the true attractor with N spikes per burst.

age. Circuits have been proposed that take advantage of this fact.[18] Even if a biological bursting neuron is not truly multistable, the shape of P indicates that the system will always have a nonmonotonicity in the contraction of the vector field about the attractor (in C_τ). This allows temporal amplification of perturbations to the system even if it has only one true attractor (Fig. 8).

In this report, we have proposed a basic dynamical mechanism for the existence of multirhythmic bursting in the biophysical models that previously demonstrated this behavior. We then explored the range of dynamics possible in circle/circle type bursting systems. Finally, we provided evidence for the existence of multirhythmic bursting in biological neurons. These experiments demonstrate a response to perturbations that is consistent with the dynamical model described herein. Further work concerning the nature of multirhythmic bursting neurons embedded within neural circuits is necessary to understand the importance of these findings in terms of short term memory.

ACKNOWLEDGMENTS

The authors thank Astrid Prinz, Jianxia Cui, and Hiroki Sayama for helpful comments. J.P.N. was supported by Georgia Tech's NSF IGERT program on Hybrid Neural Microsystems (Grant No. DGE-0333411) and an NSF Graduate Research Fellowship. Experimental and modeling work was also supported by grants from the NSF (Grant No. CBET-0348338) and NIH (Grant No. R01-HL088886), respectively, to R.J.B.

APPENDIX A: MATHEMATICAL DETAILS OF THE SIMPLE CIRCLE/CIRCLE BURSTING MODEL

1. The quadratic integrate and fire neuron model

Consider the quadratic integrate and fire model [Eq. (3)]. When u_1 is treated as a parameter,

$$\dot{v} = b_{sn} + v^2, \tag{A1}$$

where $b_{sn}=I+u_1$. A saddle node bifurcation occurs when $\sqrt{b_{sn}}=0$, indicating that the roots of the right hand side of Eq. (A1) have coalesced. When $b_{sn}<0$, these roots are real, $v_{eq}=\pm\sqrt{b_{sn}}$, and are the equilibria of Eq. (A1). When $b_{sn}>0$,

$$v(t) = \sqrt{b_{sn}}\tan(\sqrt{b_{sn}}(t+t_0)), \tag{A2}$$

which is an exact solution for the membrane potential $v(t)$.

From this, we can calculate the periodicity of spiking once the neuron has moved to the tonic regime by finding the time for $v(t)$ to go from v_r to v_c. Let t_1+t_0 be the instant that a spike begins such that $v(t_1)=v_r$ and t_2+t_0 be the instant that a spike terminates such that $v(t_2)=v_c$. From Eq. (A2)

$$v_r = \sqrt{b_{sn}}\tan(\sqrt{b_{sn}}(t_1+t_0)), \tag{A3}$$

$$v_c = \sqrt{b_{sn}}\tan(\sqrt{b_{sn}}(t_2+t_0)). \tag{A4}$$

Solving for t_1 and t_2,

$$t_1 = \left(\arctan\left(\frac{v_r}{\sqrt{b_{sn}}}\right) \Big/ \sqrt{b_{sn}}\right) - t_0, \tag{A5}$$

$$t_2 = \left(\arctan\left(\frac{v_c}{\sqrt{b_{sn}}}\right) \Big/ \sqrt{b_{sn}}\right) - t_0. \tag{A6}$$

Therefore, the interspike period (the period of a fast oscillation) is given by $T=t_1-t_2$ which matches Eq. (15).

2. Average bursting dynamics

The slow subsystem of the simple model [Eqs. (4) and (5)] is T-periodically perturbed. Each time an action potential occurs in the fast subsystem [Eq. (3)], there is an instantaneous modification of the slow variables. Let d_i represent the magnitude of this modification on a single slow variable u_i for each spike. Finding the average contribution of these modifications on the time derivative of u_i follows from the insertion of a delta function into Eq. (12),

$$\frac{1}{T(u_1)}\int_0^{T(u_1)} d_i\delta(t-T(u_1))dt = \frac{d_i}{T(u_1)}. \tag{A7}$$

The time constant ϵ is dropped in this calculation because discrete changes to the slow variables are completely removed from contributions of time constants in the continuous dynamics defined by Eqs. (4) and (5). The validity of this result is confirmed by noting that

$$\int_0^{T(u_1)} \frac{d_i}{T(u_1)}dt = \frac{d}{T(u_1)}T(u_1) = d_i. \tag{A8}$$

Therefore, when $d_i/T(u_1)$ is integrated over a single period, it produces an equivalent continuous change in the slow variables as the discrete event does instantly per single period.

APPENDIX B: EXPERIMENTAL MATERIALS AND METHODS

Aplysia californica was purchased from University of Miami Aplysia Resource Facility (Miami, FL) and maintained in a tank with filtered artificial sea water (ASW; Instant Ocean, Burlington, NC) at a temperature of about 19 °C until used. Each animal was anesthetized prior to experimentation via injection about 50% of the animal's weight of isotonic $MgCl_2$: 71.2 g $MgCl_2$ in 1 l of ASW solution containing (in mM) 460 NaCl, 10 KCl, 11 $CaCl_2$, 30 $MgCl_2$, 25 $MgSO_4$, and 10 HEPES (4-(2-hydroxyethyl)-1-piperazineethanesulfonic acid, *p*H 7.6). The animal was then pinned to a large dissection dish and opened rostrally to caudally along the dorsal midline. The abdominal ganglion was excised and pinned dorsal side up in a dish coated with Sylgard (Dow Corning, Midland, MI) in a saline solution of 30% isotonic $MgCl_2$ and 70% ASW. The sheath of connective tissue covering the neurons of the ganglion was removed with fine scissors and fine forceps. The desheathed abdominal ganglion was then perfused with high-Mg^{2+}, low-Ca^{2+} saline, containing (in mM) 330 NaCl, 10 KCl, 90 $MgCl_2$, 20

$MgSO_4$, 2 $CaCl_2$, and 10 HEPES (*p*H 7.6) to prevent synaptic transmission. Intracellular recordings were obtained using CLAMPEX8.2 software with an Axoclamp 2B amplifier (Axon Instruments, Foster City, CA) in bridge mode using a microelectrode (10–20 M Ω resistance) filled with 3*M* potassium acetate. The membrane potential was amplified and digitized with a Digidata 1322A board (Axon Instruments) at a rate of 10 kHz. Current pulses (from −0.4 to −1.5 nA) of fixed length (2–8 s) were triggered externally using a square wave produced with an AFG3021 function generator (Tektronix, Beaverton, OR) which itself was triggered by hand.

We performed experiments on 11 bursting cells from eight animals. In order for a cell to be suitable for analysis, its activity needed to be stable and stationary so we could be confident that spike addition was experimentally induced and not the result of some intrinsic variability. Therefore, we required at least seven bursts to contain the same number of spikes before a stimulation was supplied and, if a mode switch occurred, that it was maintained for seven bursts subsequent to the perturbation. Eight out of the eleven cells tested showed activity stationary enough to be analyzed, and four of these eight cells showed instances of a sustained mode switch due to perturbation. In the four cells that showed no evidence of multirhythmicity, spike addition could only be maintained for the burst directly following the perturbation and the remaining bursts contained the nominal (prestimulus) number of spikes in the active phase. In cells that did show evidence of multirhythmicity, current pulses were not consistently able to induce a switch in bursting mode but our criteria for an attractor switch was met at least one time for each of the four cells, with three out of the four cells showing multiple instances of a mode change. We saw no obvious qualitative correlation between characteristics of bursting (periodicity, duty cycle, number of spikes in the active phase, etc.) and whether a cell was capable of a mode switch in response to perturbation due to the small sample size and simplicity of our study.

[1] Y. Chagnac-Amitai and B. W. Connors, "Synchronized excitation and inhibition driven by intrinsically bursting neurons in neocortex," J. Neurophysiol. **62**, 1149 (1989).

[2] R. J. Butera, J. Rinzel, and J. C. Smith, "Models of respiratory rhythm generation in the pre-Botzinger complex. I. Bursting pacemaker neurons," J. Neurophysiol. **82**, 382 (1999).

[3] R. J. Butera, J. Rinzel, and J. C. Smith, "Models of respiratory rhythm generation in the pre-Botzinger complex. II. Populations of coupled pacemaker neurons," J. Neurophysiol. **82**, 398 (1999).

[4] L. K. Purvis, J. C. Smith, H. Koizumi, and R. J. Butera, "Intrinsic bursters increase the robustness of rhythm generation in an excitatory network," J. Neurophysiol. **97**, 1515 (2007).

[5] R. E. Plant and M. Kim, "Mathematical description of a bursting pacemaker neuron by a modification of the Hodgkin-Huxley equations," Biophys. J. **16**, 227 (1976).

[6] E. R. Kandel, *Behavioral Biology of Aplysia* (Freeman, San Francisco, 1979).

[7] J. Hounsgaard, H. Hultborn, B. Jespersen, and O. Kiehn, "Bistability of alpha-motoneurones in the decerebrate cat and in the acute spinal cat after intravenous 5-hydroxytryptophan," J. Physiol. (London) **405**, 345 (1988).

[8] H. A. Lechner, D. A. Baxter, J. W. Clark, and J. H. Byrne, "Bistability and its regulation by serotonin in the endogenously bursting neuron r15 in Aplysia," J. Neurophysiol. **75**, 957 (1996).

[9] D. Kleinfeld, F. Raccuia-Behling, and H. J. Chiel, "Circuits constructed from identified Aplysia neurons exhibit multiple patterns of persistent activity," Biophys. J. **57**, 697 (1990).

[10] T. Haberichter, M. Marhl, and R. Heinrich, "Birhythmicity, trirhythmicity and chaos in bursting calcium oscillations," Biophys. Chem. **90**, 17 (2001).

[11] A. Koseska, E. Volkov, A. Zaikin, and J. Kurths, "Inherent multistability in arrays of autoinducer coupled genetic oscillators," Phys. Rev. E **75**, 031916 (2007).

[12] J. J. Hopfield, "Neural networks and physical systems with emergent collective computational abilities," Proc. Natl. Acad. Sci. U.S.A. **79**, 2554 (1982).

[13] J. Foss, A. Longtin, B. Mensour, and J. Milton, "Multistability and delayed recurrent loops," Phys. Rev. Lett. **76**, 708 (1996).

[14] M. C. Mackey and U. an der Heiden, "The dynamics of recurrent inhibition," J. Math. Biol. **19**, 211 (1984).

[15] C. C. Canavier, D. A. Baxter, J. W. Clark, and J. H. Byrne, "Nonlinear dynamics in a model neuron provide a novel mechanism for transient synaptic inputs to produce long-term alterations of postsynaptic activity," J. Neurophysiol. **69**, 2252 (1993).

[16] R. J. Butera, "Multirhythmic bursting," Chaos **8**, 274 (1998).

[17] V. Matveev, A. Bose, and F. Nadim, "Capturing the bursting dynamics of a two-cell inhibitory network using a one-dimensional map," J. Comput. Neurosci. **23**, 169 (2007).

[18] R. J. Butera, N. McSpadden, and J. Mason, "Theory and design of a bio-inspired multistable oscillator," 2002 IEEE International Symposium on Circuits and Systems, 2002, pp. 301–304.

[19] J. Rinzel, "Bursting oscillations in an excitable membrane model," *Proceedings of the Eighth Dundee Conference on Ordinary and Partial Differential Equations* (Springer, Berlin, 1985).

[20] J. Rinzel and Y. S. Lee, "Dissection of a model for neuronal parabolic bursting," J. Math. Biol. **25**, 653 (1987).

[21] G. B. Ermentrout and N. Kopell, "Parabolic bursting in an excitable system coupled with a slow oscillation," SIAM J. Appl. Math. **46**, 233 (1986).

[22] E. M. Izhikevich, "Neural excitability, spiking and bursting," Int. J. Bifurcation Chaos Appl. Sci. Eng. **10**, 1171 (2000).

[23] E. M. Izhikevich, *Dynamical Systems in Neuroscience: The Geometry of Excitability and Bursting*, Computational Neuroscience (MIT Press, Cambridge, MA, 2007).

[24] J. Guckenheimer, "Toward a global theory of singularly perturbed systems," Progress in Nonlinear Differential Equations and Their Applications **19**, 213 (1996).

[25] Practically, the placement of Σ_c entails an error resulting from the assumption that fast and slow time scales are infinitely separated. In order to find the value of u_1 that truly separates spiking and resting states, we carried out numerous numerical simulations in the region of state space where contraction was balanced to determine the lowest value of u_1 that supports a spiking event.

[26] L. S. Pontryagin and L. V. Rodygin, "Periodic solution of a system of ordinary differential equations with a small parameter in the terms containing derivatives," Sov. Math. Dokl. **1**, 611 (1960).

[27] C. C. Canavier, J. W. Clark, and J. H. Byrne, "Simulation of the bursting activity of neuron r15 in Aplysia: Role of ionic currents, calcium balance, and modulatory transmitters," J. Neurophysiol. **66**, 2107 (1991).

[28] R. Bertram, "A computational study of the effects of serotonin on a molluscan burster neuron," Biol. Cybern. **69**, 257 (1993).

[29] R. J. Butera, J. W. Clark, C. C. Canavier, D. A. Baxter, and J. H. Byrne, "Analysis of the effects of modulatory agents on a modeled bursting neuron: Dynamic interactions between voltage and calcium dependent systems," J. Comput. Neurosci. **2**, 19 (1995).

[30] W. B. Adams, "Slow depolarizing and hyperpolarizing currents which mediate bursting in Aplysia neurone r15," J. Physiol. **360**, 51 (1985).

[31] C. C. Canavier, D. A. Baxter, J. W. Clark, and J. H. Byrne, "Multiple modes of activity in a model neuron suggest a novel mechanism for the effects of neuromodulators," J. Neurophysiol. **72**, 872 (1994).